ELSEVIER

Catalysis Today 38 (1997) 483–492

CATALYSIS TODAY

Nickel hydroxide electrocatalysts for alcohol oxidation reactions: An evaluation by infrared spectroscopy and electrochemical methods

Andrzej Kowal[a], Simon N. Port[b], Richard J. Nichols[b,*]

[a]The Institute of Catalysis and Surface Chemistry, Polish Academy of Sciences, Krakow, Poland
[b]Department of Chemistry, The University of Liverpool, Liverpool L69 3BX, UK

Abstract

We have investigated the electrochemical oxidation of four alcohols (methanol, 1-, 2- and tertiary butanol) at Ni hydroxide electrodes in alkaline electrolytes. In situ FTIR spectroscopy and electrochemical methods have been used to examine these oxidation reactions. Oxidation of the primary and secondary alcohols commences in the potential region where it is proposed that multi-layers of NiOOH are formed on the electrode surface; while no reaction occurs with tertiary butanol. Methanol oxidation occurs in two stages, with predominantly formate being formed in the potential window 0.36–0.44 V (vs. SCE), followed by further oxidation to carbonate at potentials above approx. 0.45 V. Butanoate is the only detected reaction product for 1-butanol electrooxidation in the potential range 0.36–0.5 V. The oxidation of 2-butanol is more complex. In the lower potential range (0.36–0.44 V) the major reaction product is butanone, which is further oxidised at higher potentials to either acetate or a mixture of propanoate and formate (or carbonate). In addition, rate constants have been determined for the first stage of the electrochemical oxidation of all the alcohols investigated. © 1997 Elsevier Science B.V.

Keywords: Nickel hydroxide; Alcohol; Oxidation; In situ FTIR; Electrochemistry

1. Introduction

Catalysts in the form of electrode surfaces provide the added dimension of the electrode potential which can be used to control the catalyst reactivity and in some cases selectivity. However, reactions at electrocatalysts are inherently more difficult to characterise than their gas phase counterparts, due to the greater difficulty of directly detecting products, intermediates and adsorbates formed at electrochemical interfaces. This study here focuses on nickel hydroxide electrocatalysts and the electrooxidation of alcohols. Such electrocatalysts currently have applications in the electrochemical transformation of alcohols to organic acid anions [1–6] which is of use, for instance, in vitamin C synthesis [3,5,6].

It is known that the mechanism of the oxidation of alcohols on Ni/NiOOH electrodes depends on the position of the hydroxyl group in the molecule [2]. The oxidation of primary alcohols at Ni/NiOOH electrodes in alkaline medium leads to the formation of organic acids:

$$RCH_2OH \xrightarrow{NiOOH-4e} RCOOH \quad (1)$$

In the process of the oxidation of secondary alcohols ketones are formed:

---

*Corresponding author. Tel. : (44-151) 794-3533; Fax: (44-151) 794-3588; e-mail: nichols@liv.ac.uk

0920-5861/97/$32.00 © 1997 Elsevier Science B.V. All rights reserved.
PII S0920-5861(97)00049-7

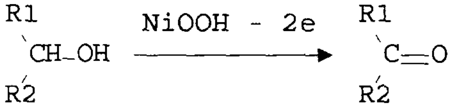

$$\mathrm{R1(R2)CH{-}OH} \xrightarrow{\mathrm{NiOOH}\ -\ 2e} \mathrm{R1(R2)C{=}O} \qquad (2)$$

while tertiary alcohols do not oxidise [1–4].

A general mechanism of the oxidation of primary alcohols was proposed by Fleischmann et al. [1,2].

- Oxidation of surface $Ni(OH)_2$ to NiOOH:

$$OH^- + Ni(OH)_2 \underset{k_{E'}}{\overset{k_E}{\rightleftarrows}} NiOOH + H_2O + e^- \qquad (3)$$

- Adsorption of alcohol:

$$RCH_2OH_{sol.} \underset{k_{A'}}{\overset{k_A}{\rightleftarrows}} RCH_2OH_{ads.} \qquad (4)$$

- Hydrogen-abstraction reaction:

$$RCH_2OH_{ads.} + NiOOH \underset{k_c}{\overset{rds}{\rightarrow}} \underset{\text{intermediate}}{RC^{\bullet}HOH} + Ni(OH)_2 \qquad (5)$$

- Subsequent (fast) oxidation of adsorbed intermediate:

$$RCH^{\bullet}OH + H_2O \overset{fast}{\rightarrow} RCOOH + 3e + 3H^+ \qquad (6)$$

or

$$RCH^{\bullet}OH + 3NiOOH + H_2O \overset{fast}{\rightarrow} RCOOH + 3Ni(OH)_2 \qquad (7)$$

Fleischmann et al. [1] have analysed the current vs. potential (polarisation) curves for the oxidation of various alcohols on Ni-electrodes. Two regions of the polarisation curve were identified: a rising current region followed by a current plateaux region at more positive potentials. In the rising current region the reaction was determined to be first order in both the alcohol and hydroxide ion concentration and a Tafel slope of $(60\ \mathrm{mV})^{-1}$ was measured. This region was identified as a Tafel region. In the current plateaux region the reaction was also found to be first order in alcohol concentration, but zero order with respect to the hydroxide-ion concentration. Notably, the current on the plateaux of these waves were much smaller than would be expected for a diffusion controlled process. Further experiments with a rotating disc electrode indicated that the currents were independent of the rotation speed of the electrodes and hence kinetically controlled [1]. Hence this current plateaux region was identified as a kinetically controlled limiting current region.

According to this mechanism the current in the Tafel region is expressed as [1]

$$i = nFA\alpha \frac{k_C k_E k_A}{k_E' k_A'} C_{alc.} C_{OH^-} \exp\left(\frac{F\phi}{RT}\right) \qquad (8)$$

where ϕ is the electrode potential, F the Faraday constant, n the number of electrons, A the electrode area, β roughness factor, $C_{alc.}$ the concentration of alcohol and C_{OH^-} is the concentration of OH^-; and the kinetically controlled limiting current is given by the equation:

$$i = nFA\beta \frac{k_C k_A C_{alc.}}{k_A'} = nFAKC_{alc.}, \qquad (9)$$

where

$$k = \frac{\beta k_C k_A}{k_A'}. \qquad (10)$$

This rate constant k is a mixed constant for formation of the oxidised compound at the given electrode. As can be seen from Eq. (10) the mixed rate constant contains three factors: (a) the roughness factor of the electrode surface, β; (b) the equilibrium constant for the adsorption of the organic molecule, $K_A = k_A/k_A'$ and (c) the rate constant for the hydrogen-abstraction reaction [1].

Extensive work has been conducted on the electrooxidation of alcohols, particularly with active noble metal electrodes, owing to their possible use in fuel cells [7,8]. There has also been a sizeable body of spectroscopic work aimed at characterising products and adsorbed intermediates formed during alcohol oxidation, largely on noble metal electrodes [8]. The identification by in situ infrared spectroscopy of adsorbed CO as the "poisoning intermediate" during the oxidation of alcohols and other small organic molecules is particularly noteworthy here [9]. Much emphasis has been placed on investigating the effect of surface structure and electrolyte composition on the formation of adsorbed CO from a wide variety of small organic molecules [8]. A number of other studies have focused on the so-called reactive intermediates resulting from small organic molecule chemisorption [10]. These reactive intermediates are more weakly adsorbed than CO and are consequently more readily oxidised from the surface. For instance, there is IR-spectroscopic evidence for adsorbed COH being formed during methanol oxidation on active platinum electrodes [11].

As well as enabling the identification of adsorbates, in situ IR spectroscopy also particularly lends itself to the detection of soluble reaction products formed during electrolysis. Due to experimental constraints FTIR spectra can only be obtained for specially designed thin layer cells, where the electrolyte thin layer is typically between about 1 and 100 μm thick. For instance, Weaver et al. [12] have investigated the products formed from the thin layer voltammetric oxidation of methanol, ethanol and isopropanol on platinum by means of FTIR spectroscopy. Electrooxidation of these alcohols were investigated in both pure non-aqueous and concentrated aqueous environments [12]. For anhydrous methanol and ethanol electrooxidation in 0.1 M $LiClO_4$ partial oxidation products were identified by IR spectroscopy, including 1,1-dimethoxymethane and 1,1-diethoxyethane and methyl formate. No adsorbed CO or CO_2 product was observed [12]. The addition of small quantities of aqueous $HClO_4$ led to marked changes in the mechanism of electrooxidation and the distribution of products with, in the case of methanol oxidation, adsorbed CO and CO_2 appearing [12]. Other groups have also used FTIR spectroscopy to identify soluble reaction products. Notably, Morallón et al. [13] have identified formate and CO_2 as soluble reaction products of methanol oxidation on platinum in alkaline media.

Far fewer IR-spectroscopic investigations have been directed towards the behaviour of nickel or nickel hydroxide electrocatalyts, despite the significant technological interest in these electrodes. In this respect, Koga and Hori [14] have studied the electroreduction of CO_2 at nickel electrodes. They assigned a band at about 1900 cm^{-1} to adsorbed CO formed by CO_2 reduction [14]. Zhao et al. [15] have also examined adsorbed CO on nickel electrodes. However, the emphasis of this study is on the electrochemical oxidation of the CO adsorbate in alkaline solutions, with the formation of soluble carbonate. Other IR studies have focused on nickel hydroxide phases formed on nickel electrode surfaces [16,17].

In this paper we investigate methanol and 1-, 2- and tertiary butanol electrooxidation. The course of the electrooxidation has been monitored by in situ infrared (IR) spectroscopy, voltammetry and standard analytical methods. IR spectroscopy is particularly useful here, in that it enables direct chemical identification of reaction products. This allows an assessment of the selectivity of nickel hydroxide electrocatalysts towards the formation of certain oxidation products from alcohols.

2. Experimental

2.1. Electrochemical studies

In order to obtain a hydroxide layer of a certain thickness the nickel electrode was subjected to cyclic oxidation–reduction between −0.25 and 0.55 V vs. SCE for 15 min. The apparent electroreduction charge density related to the geometric area of the electrode, measured after this pre-treatment, was Q_r=7.8 mC/cm^2.

The average thickness (L) of the layer, can be determined according to the equation given by Arvia [18]:

$$L = x \times Q_r,$$

where x is a constant determined by Arvia [18] as 4.33 nm/(mCcm^{-2}).

Thus Q_r=7.8 mC/cm^2 gives an average layer thickness of about 34 nm. All electrode potentials were measured and are quoted vs. the SCE reference electrode.

2.2. IR spectroscopy

A polycrystalline nickel disc electrode, 12 mm in diameter and 2 mm thick was used for the in situ IR spectroscopy experiments. This Ni electrode was prepared by polishing with successive grades of alumina powder down to 0.05 μm. Prior to the experiments this electrode was pre-treated to develop a nickel hydroxide surface layer. This pre-treatment involved cycling the electrode potential twice from −0.25 to +0.55 V. It has been previously reported that potential cycling in this range leads to formation of a multi-layer hydrated Ni oxide layer [18].

In situ FTIR spectroscopy has been used here to monitor the reaction products as a function of electrode potential. Potential difference IR spectra were obtained using the subtractively normalised interfacial Fourier transform spectroscopy technique (SNIFTIRS) [19,20]. A three electrode cell with a CaF_2 window (spectral cut-off below 1000 cm^{-1}) was employed for all spectroscopic experiments. After preparation and potential cycling pre-treatment the solid Ni electrode was aligned against the IR window. The thin layer cell thus formed usually has a thickness in the order of between a few microns to several tens of microns [21]. The potential was controlled with a potentiostat and waveform generator (HiTek; UK, DT2101 and PPR1); the potentiostat was switched between two pre-set potentials and IR reflectance spectra collected at each potential. Before spectral collection the solutions were purged with nitrogen (oxygen free, BOC). A dry air purged FTIR spectrometer (BioRad FTS40) with a liquid nitrogen cooled mercury cadmium telluride (MCT) detector was used for all the SNIFTIRS experiments. P-polarised radiation was employed. Normalised spectra were obtained by subtracting two spectra (R_2–R_1) obtained for different potentials and dividing this difference by R_1, the reference spectrum. Thus, the normalised change in reflectance is given by

$$\Delta R/R = (R_2 - R_1)/R_1.$$

Consider that a new molecular species is formed at potential 2 (E_2) which is not present at E_1 and that this species gives rise to new IR absorption peaks. These peaks will point downwards in the $\Delta R/R$ (SNIFTIRS) spectrum, since increased IR absorption at E_2 is equivalent to decreased reflectivity at E_2, i.e. $(R_2-R_1)/R_1<1$. In other words, in simple situations negative going bands are related to species which are in excess at E_2, while positive going ones correspond to species in excess at the reference potential (E_1). The signal-to-noise ratio of the IR spectrum was improved by collecting a number of interferograms at each potential.

3. Results and discussion

3.1. Electrochemical data

Figs. 1–3 show the polarisation curves for methanol, 1-butanol and 2-butanol oxidation obtained at different concentrations of alcohols by a potentiostatic method, starting from 0.285 V vs. SCE. The potential of the electrode was shifted in 25 mV steps after waiting 10 min at each potential; during this period a steady-state was attained.

It can be seen that the current plateau is observed for these three alcohols, but in the case of methanol and

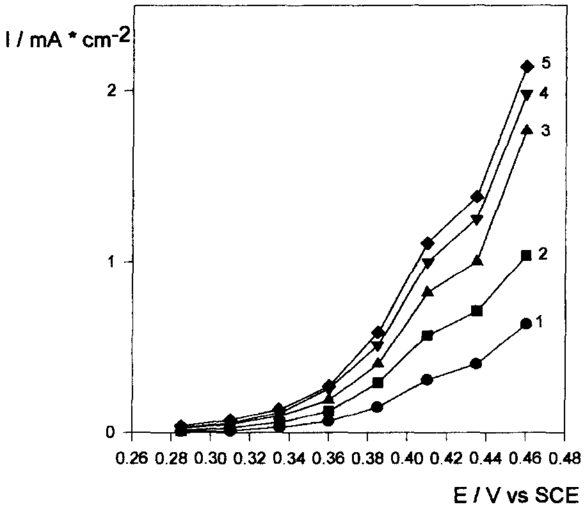

Fig. 1. Steady-state polarisation curves for methanol oxidation in 1 M KOH at a Ni/NiOOH electrode; the concentration of alcohol: 1, 0.1 M; 2, 0.2 M; 3, 0.3 M; 4, 0.4 M; 5, 0.5 M.

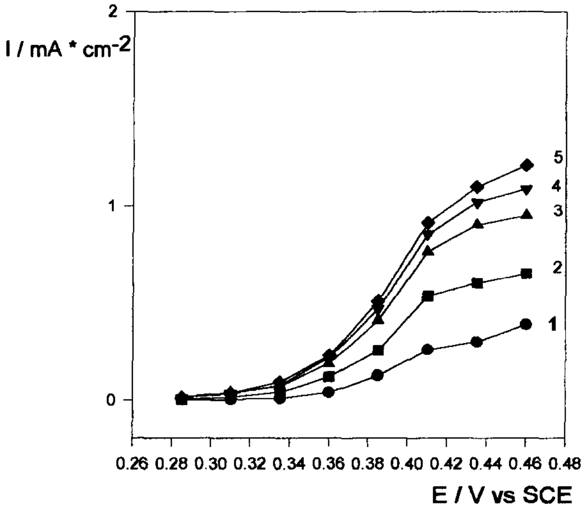

Fig. 2. Steady-state polarisation curves for 1-butanol oxidation in 1 M KOH at a Ni/NiOOH electrode; the concentration of alcohol: 1, 0.1 M; 2, 0.2 M; 3, 0.3 M; 4, 0.4 M; 5, 0.5 M.

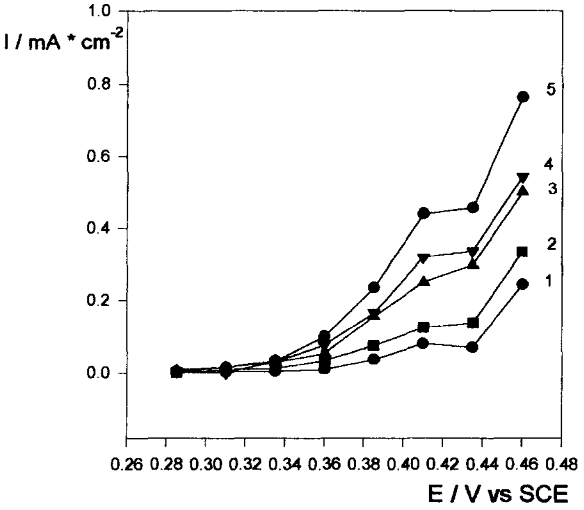

Fig. 3. Steady-state polarisation curves for 2-butanol oxidation in 1 M KOH at a Ni/NiOOH electrode; the concentration of alcohol: 1, 0.1 M; 2, 0.2 M; 3, 0.3 M; 4, 0.4 M; 5, 0.5 M.

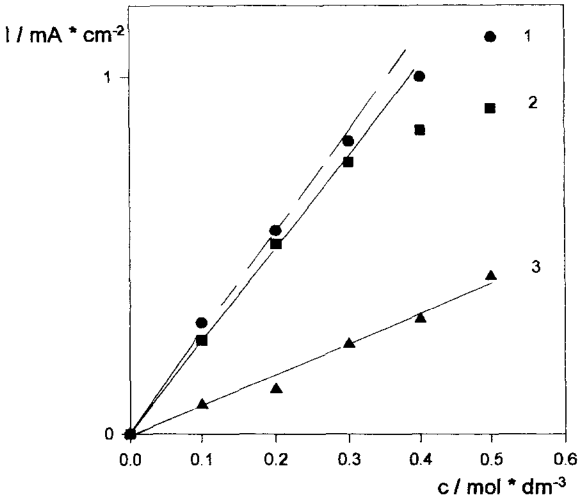

Fig. 4. Dependencies of steady-state limiting current density on alcohol concentration; 1, methanol; 2, 1-butanol; 3, 2-butanol. Taken for E=0.41 V.

2-butanol the plateau is followed by an increase in current density indicating the occurrence of a second oxidation step. The steady-state current–concentration plots, measured at potentials in the current plateau region are presented in Fig. 4. The rate constant k for the oxidation of the investigated alcohols at the Ni/NiOOH electrode are calculated according to Eq. (9) and are summarised in Table 1. As discussed in Section 1 the measured rate constant k is a mixed rate constant having contributions from the equilibrium constant for alcohol adsorption, the electrode roughness and the rate of hydrogen-abstraction from the adsorbed alcohol.

Table 1
Rate constants for the electrochemical oxidation of the investigated alcohols at Ni/NiOOH electrodes

Alcohol	k (cm s^{-1})$\times 10^6$	E (V) vs. SCE
Methanol	7.5	0.41
1-Butanol	6.8	0.41
2-Butanol	3.6	0.41
t-Butanol	0	0.41

It can be concluded that the rate constant for the reaction between nickel electrodes and the primary alcohols methanol and 1-butanol is about two times larger than that for the secondary butanol. It can be also deduced that the electrochemical oxidation of methanol and 2-butanol is more complex than in the case of 1-butanol. The subsequent oxidation of these two alcohols is observed at higher potentials (E>0.44 V).

4. In situ FTIR results

4.1. Electrooxidation of methanol

Fig. 5 shows in situ FTIR spectra recorded for a polycrystalline nickel electrode in 1 M NaOH with 0.5 M methanol. Prior to the spectroscopic measurements the electrode potential was cycled twice between −0.25 and 0.55 V (vs. SCE), to develop the nickel hydroxide layer. The reference spectrum was recorded at −0.25 V, a potential at which no electrooxidation occurs. Spectra were recorded at this reference potential and then the potential was switched to the second (more positive) potential limit, where spectra were also recorded. The potential difference spectrum was calculated from the respective spectra at these two potential limits. Bands pointing upwards correspond to species in excess at the reference potential, while downwards pointing bands correspond to species in excess at the positive potential

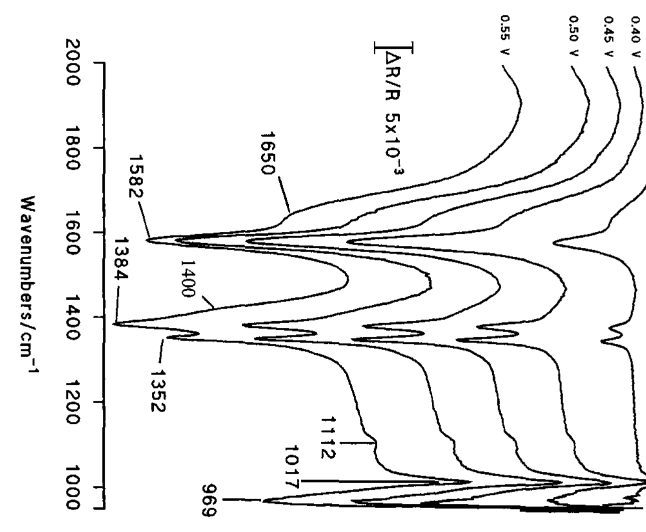

Fig. 5. In situ potential difference IR spectra (SNIFTIRS) of the polycrystalline Ni electrode in 1 M NaOH with 0.5 M methanol. The reference potential was −0.25 V and the other potential limit of the difference spectra is shown next to each spectrum. Downward pointing bands correspond to IR absorbance by species in excess at the positive potential limit. Prior to recording the spectra the electrode potential was cycled between −0.25 and +0.55 V to develop the hydrated nickel oxide layer.

limit. The positive potential limit is marked for each of the difference spectra in Fig. 5.

In the spectral series shown in Fig. 5 there is only one pronounced positive band at 1017 cm^{-1}. From Table 2, methanol in aqueous NaOH shows a similar strong band at 1017 cm^{-1}. This corresponds to the C–O stretch of methanol [22]. The positive sign of the band implies that methanol is in excess at the reference potential, in other words it reacts to form another species at the positive potential limit. The intensity of this band gives an indication of the potential dependence of the reaction. Thus, there is no apparent band when the positive potential limit is +0.3 V, but a small one appears when the positive limit is increased to 0.35 V. The potential of +0.35 V lies just at the foot of the current peak corresponding to oxide formation in the cyclic voltammogram of Ni in 1 M NaOH.

Table 2
Tabulated IR bands frequencies in cm^{-1} for alcohols and related oxidation products in the region from 2000 to 950 cm^{-1}

Compound																	
Methanol[c]														1054 (m)	1034 (s)	1013 (sh)	
Methanol[a]								1318 (m)						1085 (w)		1017 (s)	
Butan-1-ol[c]				1463 (s)		1379 (s)					1216 (w)		1114(s)	1073 (s)	1036 (s)	1011 (m)	992 (m)
Butan-2-ol[c]		1654 (b)		1459 (s)	1418 (m)	1376 (s)		1328 (m)	1300 (sh)	1254 (m)		1153 (s)	1100 (s)		1032 (s)		992 (s)
t-Butanol[c]		1655 (b)		1473 (s)		1382 (s)	1365 (s)			1241 (s)	1202 (sb)				1023 (s)		
Butan-2-one[c]	1713 (s)	1653 (b)		1457 (s)	1418 (s)		1365 (sb)			1256 (m)	1205 (sh)	1169 (s)		1086 (s)			996 (m)
Butan-2-one[a]	1702 (s)	1654 (s)		1459 (m)	1419 (m)		1370 (sb)			1260 (w)	1210 (sh)	1181 (s)		1088 (w)			997 (w)
Formate[a]		1650 (sb)	1586 (sb)			1385 (s)	1352 (s)										
Propanoate[a]		1650 (sb)	1550 (s)	1467 (m)	1415 (s)		1374 (m)		1300 (m)					1079 (m)			
Carbonate[a]		1650 (sb)				1400 (sb)											
Acetate[a]		1650 (sb)	1559 (s)		1416 (s)											1019 (w)	

Abbreviations: s, *strong*; sh, *shoulder*; b, *broad*; sb, *strong broad*; m, *medium*; w, *weak*.
Data taken from transmission spectra with CaF_2 plates.
Measurements are for [c]neat liquid or [a]solutions in aqueous alkaline (NaOH) media.

The downwards pointing bands appear at 1650, 1582, approx. 1400 (broad shoulder), 1384 and 1352 cm^{-1}. The band at 1650 cm^{-1} can be assigned to water deformation, and it arises from changes in the water structure in the thin layer. The bands at 1582, 1384 and 1352 cm^{-1} correlate very well with three characteristic bands of formate, seen in transmission spectra of formate in aqueous NaOH. The 1582 cm^{-1} band is assigned to ν_a(COO), the 1384 cm^{-1} band to δ(CH) or p_r(COO) and the 1352 band to ν_s(COO) of formate [23]. The broad shoulder at about 1400 cm^{-1} is most pronounced for higher positive potential limits. It is also interesting to compare the relative intensities of the three characteristic formate bands with this shoulder, for the spectra with the positive limits of 0.40, 0.45, 0.50 and 0.55 V, respectively. As the positive limit is increased the 1400 cm^{-1} shoulder becomes more dominant. Carbonate (in 1 M NaOH) has a predominant band at about 1400 cm^{-1}. Hence, a realistic assignment of this band is to carbonate which is formed by further oxidation of formate. The fact that the relative intensity of the carbonate band increases from 0.4 to 0.55 V implies that the selectivity of the nickel hydroxide electrocatalyst with respect to formate formation decreases at the higher potentials.

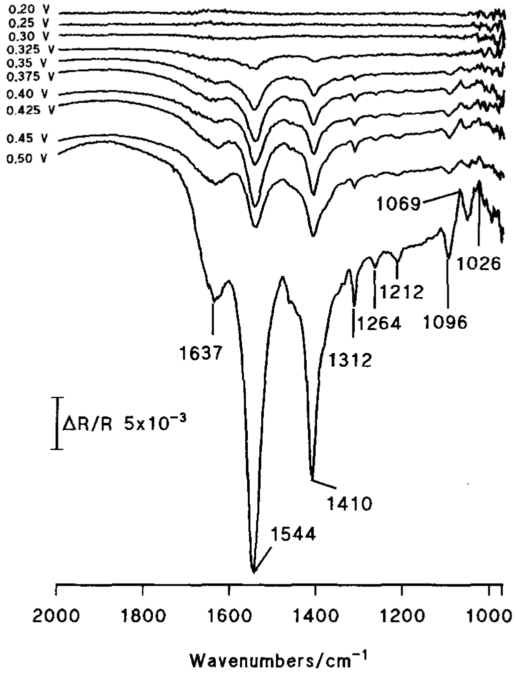

Fig. 6. In situ potential difference IR spectra of the polycrystalline Ni electrode in 1 M NaOH with 0.5 M butan-1-ol. All other conditions are the same as Fig. 5.

4.2. 1-Butanol

Spectra for a polycrystalline Ni electrode in 1 M NaOH with 0.5 M 1-butanol are shown in Fig. 6. As for the methanol experiments, the electrode was cycled two times between −0.25 and 0.55 V to develop the nickel hydroxide surface film. A reference potential of −0.25 V was also chosen. Upwards pointing peaks are seen at 1069 and 1026 cm^{-1}. These correspond well with bands observed in the transmission spectra of 1-butanol (see Table 2). Downwards pointing bands were seen to develop as the positive limit was increased from +0.35 to +0.5 V. The two most pronounced bands at 1544 and 1410 cm^{-1} fall at frequencies characteristic of the asymmetrical and symmetrical (COO) stretches of carboxylate anions [23]. These spectra are consistent with butanoate being formed by electrooxidation of 1-butanol. As for methanol, the lowest positive potential limit where bands for oxidation products appear is about +0.35 V. Bands characteristic of either aldehydes or formate cannot be seen in the spectra, even at the highest positive potential limit, indicating that there is a good selectivity towards formation of the organic acid anion from 1-butanol.

4.3. 2-Butanol

Spectra for a polycrystalline Ni electrode in 1 M NaOH with 0.5 M 2-butanol are shown in Fig. 7. The electrode was prepared in the same fashion as for the methanol and 1-butanol experiments. The upwards pointing bands, at 1105, 1031 and 994, are also seen in the transmission spectra of 2-butanol (see Table 2), and this points to 2-butanol being in excess at the reference potential of −0.25 V. The downwards pointing bands are seen at 1698, 1635, 1555, 1414, 1371 and 1185 cm^{-1}. These bands correspond to oxidation products of 2-butanol. The band at 1698 cm^{-1} is the most characteristic and it can be assigned to the first oxidation product of 2-butanol, which is butan-2-one. Notice that hydrogen bonding in aqueous solution shifts this C=O stretching vibration from 1713 cm^{-1} for the neat solution of butan-2-one, to 1702 cm^{-1} in

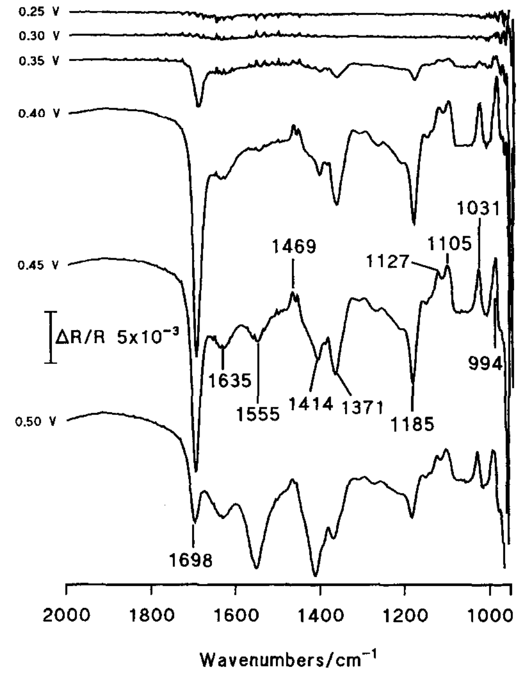

Fig. 7. In situ potential difference IR spectra of the polycrystalline Ni electrode in 1 M NaOH with 0.5 M butan-2-ol. All other conditions are the same as Fig. 5.

aqueous NaOH solution. By comparison with transmission spectra for 2-butanone in aqueous NaOH (Table 2) the other strong bands in the in situ FTIR spectra which can be assigned to this ketone are at 1371 and 1185 cm^{-1}. All these ketone bands decrease in intensity as the positive potential limit is increased from 0.40 to 0.45 V and then further to 0.50 V. By 0.50 V the ketone bands have fallen to a fraction of their maximum intensity at 0.40 V and new bands are clearly seen, at 1555 and 1414 cm^{-1}. These new bands arise from the further oxidation of the ketone. Butan-2-one can be oxidatively cleaved to form either acetate (a) or propanoate and formate (b):

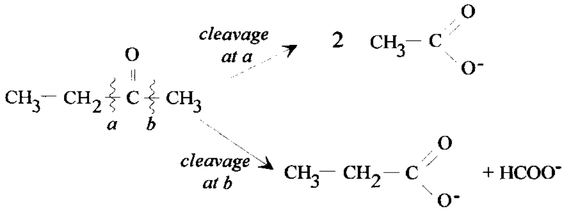

The two new bands at 1555 and 1414 cm^{-1} occur at frequencies observed for the asymmetric and symmetric stretches of organic acid anions. Therefore, the spectra are consistent with the formation of carboxylate species at the higher positive potentials. However, we cannot distinguish whether the major product is either acetate or a mixture of propanoate and formate (or carbonate formed by further oxidation of formate).

4.4. *Tertiary butanol*

In situ FTIR spectra have been recorded under similar conditions for the nickel electrode in 1 M NaOH with 0.5 M tertiary butanol. Neither bands corresponding to loss of the alcohol nor bands corresponding to the formation of oxidation products were seen. This resilience of tertiary butanol to electrooxidation is not surprising since, in contrast to the other alcohols, it lacks an α-hydrogen.

5. Conclusions

The electrooxidation of four alcohols was studied on polycrystalline Ni/NiOOH electrodes in alkaline media using electrochemical and IR spectroscopic methods. The following conclusions can be made about the electrooxidation of the investigated alcohols:

(a) Electrooxidation of methanol, 1-butanol and 2-butanol commences at about 0.36–0.38 V vs. SCE in 1 M KOH. This is in the region where it is reported that multi-layer NiOOH films develop on the electrode surface [16]. Tertiary butanol is resistant to oxidation.

(b) The steady-state polarisation curves for methanol, 1-butanol and 2-butanol show a sharply rising current between about 0.36 and 0.41 V. This is followed by a plateau region between about 0.41 and 0.44 V. This is assigned to a kinetically controlled limiting current region. Polarisation curves have been recorded at a range of alcohol concentrations from 0.1 to 0.5 M. The steady current measured at 0.41 V has been plotted against alcohol concentration for the investigated alcohols. Using the expression for the plateau current derived by Fleischmann et al. [1,2] rate constants k for the oxidation of the alcohols were calculated. The rate constants derived are 7.5 (methanol), 6.8 (1-butanol), 3.6 (2-butanol) and 0 (tertiary butanol)$\times 10^{-6}$ cms^{-1} (all measured at 0.41 V vs. SCE). The measured rate constant, k, is a mixed rate constant having contributions from the equilibrium constant for alcohol adsorption, the electrode roughness and the rate of hydrogen-abstraction from the adsorbed alcohol.

(c) Both methanol and 2-butanol show a sharply rising current following (>0.44 V) the current plateau. This is related to subsequent electrooxidation of these two alcohols. 1-Butanol does not show this feature, indicating that the electrochemical oxidation of the methanol and 2-butanol is more complex than the case of 1-butanol.

(d) In 1 M aqueous NaOH the major product of methanol oxidation at Ni electrodes, as identified by FTIR, is formate. However, on increasing the electrode potential above about 0.45 V (vs. the saturated calomel reference electrode, SCE), selectivity decreases with formate being further oxidised to form carbonate. This is consistent with the polarisation curves which indicate two stages to the oxidation.

(e) Under similar conditions the only product detected by FTIR spectroscopy for 1-butanol oxidation was butanoate, while not surprisingly tertiary butanol is resilient to oxidation to potentials of at least 0.55 V (vs. SCE).

(f) FTIR spectroscopy shows that the behaviour of 2-butanol is somewhat more complex. At lower electrode potentials (approx. 0.3–0.4 V) butanone is the major product. At more positive potentials (approx. 0.4–0.55 V) carboxylate species are detected by IR spectroscopy, indicating oxidative cleavage of one (or both) of the C–C bonds adjacent to the ketone. In this case the IR spectroscopic data could not enable us to discern whether either acetate or a mixture of propanoate and formate (and carbonate) are formed.

Summarising the results for the electrooxidation of the investigated alcohols at Ni/NiOOH in 1 M alkaline electrolytes:

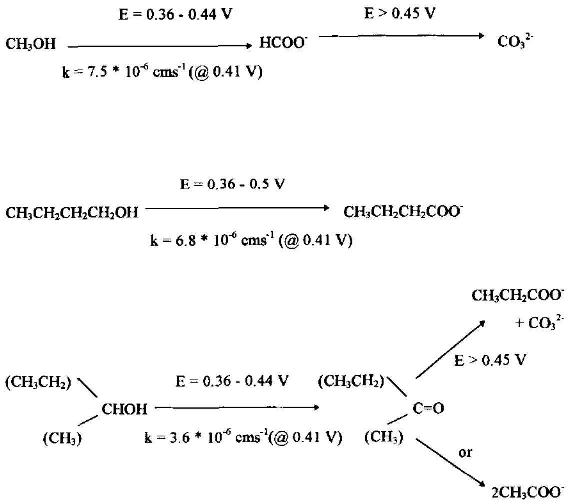

$(CH_3)_3COH$ no reaction.

Acknowledgements

One of us (A.K.) would like to thank the Royal Society for financial support during an ESEP study visit in Liverpool.

References

[1] M. Fleischmann, K. Korinek, D. Pletcher, J. Chem. Soc., Perkin Trans. 2 (1972) 1396.

[2] M. Fleischmann, K. Korinek, D. Pletcher, J. Electroanal. Chem. 31 (1971) 39.

[3] G. Vértes, G. Horányi, F. Nagy, Croat. Chem. Acta 44 (1972) 21.

[4] H.-J. Schäfer, Top. Curr. Chem. 142 (1987) 101.

[5] P.M. Robertson, P. Berg, H. Reimann, K. Schleich, P. Seiler, J. Electrochem. Soc. 130 (1983) 591.

[6] A. Kowal, J. Haber, M. Czerwenka, M. Adamus, J. Bujak, A. Krawiec, B. Ziobro, Polish Patent No. 148 144 (1989).

[7] R. Parsons, T. VanderNoot, J. Electroanal. Chem. 257 (1988) 9.

[8] M.P. Soriaga, Structure of electrified interfaces, in: P.N. Ross, J. Lipkowski (Eds.), Series: Frontiers in Electrochemistry, vol. 2, ch. 4, VCH, New York, NY, 1992, pp. 103–152.

[9] B. Beden, A. Bewick, K. Kunimatsu, C. Lamy, J. Electroanal. Chem. 121 (1981) 343.

[10] R.J. Nichols, Adsorption of molecules at metal electrodes, in: P.N. Ross, J. Lipkowski (Eds.), Series: Frontiers in Electrochemistry, vol. 1, ch. 7, VCH, New York, NY, 1992, pp. 347–389.

[11] R.J. Nichols, A. Bewick, Electrochim. Acta 33 (1988) 1691–1694.

[12] P. Gao, S-C. Chang, Z Zhou, M. Weaver, J. Electroanal. Chem. 272 (1989) 161.

[13] E. Morallón, A. Rodes, J.L. Vazquez, J.M. Pérez, J. Electroanal. Chem. 391 (1985) 149.

[14] O. Koga, Y. Hori, Denki Kagaku 61 (1993) 812.

[15] M. Zhao, K. Wang, D.A. Scherson, J. Phys. Chem. 97 (1993) 4488.

[16] B. Beden, A. Bewick, Electrochim. Acta 33 (1988) 1695.

[17] A. Šurca, B. Orel, B. Pihlar, P. Bukovec, J. Electroanal. Chem. 408 (1996) 83.

[18] A. Visintin, W.E. Triaca, A.J. Arvia, J. Appl. Electrochem. 26 (1996) 493.

[19] S. Pons, T. Davidson, A. Bewick, J. Electroanal. Chem. 160 (1984) 63.

[20] A. Bewick, S. Pons, in: R.J.H. Clark, R.E. Hester (Eds.), Advances in Infrared and Raman Spectroscopy, vol. 12, 1985.

[21] K. Ashley, S. Pons, Chem. Rev. 88 (1988) 673.

[22] D.H. Williams, I. Fleming, Spectroscopic Methods in Organic Chemistry, 3rd ed., McGraw-Hill, New York, NY, 1980.

[23] K. Nakomoto, Infrared and Raman Spectra of Inorganic and Coordination Compounds, Wiley, New York, NY, 1986.